

## Reduction of Cross-Field Plasma Transport in Tokamaks due to Power Input Redistribution and Sheared Flow Profile Modification

V.P. Pastukhov, N.V. Chudin

RRC «Kurchatov Institute», 123182 Moscow, Russian Federation

e-mail contact of main author: past@nfi.kiae.ru

**Abstract.** Reduction of low-frequency (LF) turbulence and the associated anomalous cross-field plasma transport in tokamaks due to redistribution of ECH power input and controlled formation of sheared flow profiles is studied theoretically. Various scenarios of transitions to improved confinement regimes were analyzed and simulated numerically using a cylindrical model of tokamak. A fast decrease of heat flux in the core plasma region to the neoclassical value was obtained in a scenario when a significant part (40-90%) of ECH power input initially localized near the surface  $q=1$  was switched over closer to the plasma edge. A considerable weakening of LF turbulence and an appreciable increase of plasma life-time were observed as well, while the relative plasma pressure gradient remained almost unchanged. Transient regimes with controlled modification of sheared flows profiles were also simulated. It is shown that presence of high vorticity layer in the sheared flow profile can appreciably modify the structure of LF turbulence leading to a decrease of cross-field transport.

### 1. Introduction

Anomalous transport of particles and energy is one of the crucial problems in magnetic plasma confinement for fusion. As a rule the anomalous transport is associated with plasma fluctuations driven by various kinds of drift instabilities (see, e.g., [1, 2]). Due to relatively small transverse scales of the fluctuations, the anomalous transport is conventionally discussed in terms of diffusion approximation with local transport coefficients. However, many recent experiments have shown that low-frequency (LF) turbulence and the associated anomalous cross-field plasma transport observed in various magnetic confinement systems with different magnetic field topologies and plasma parameters (tokamaks [3-5], stellarators [6, 7], tandem mirrors [8, 9], etc.) exhibit rather common features, which cannot be appropriately described in terms of diffusive approximation with local transport coefficients. Many experiments show presence of dominant large-scale quasi-2D nonlinear vortex-like structures in magnetized plasmas. Very impressive results on generation and modification of such structures in a presence of sheared plasma rotation were recently obtained in GAMMA 10 tandem mirrors experiments [8, 9].

Direct computer simulation of the nonlinear plasma dynamics seems to be an appropriate method of theoretical study of such quasi-2D structured turbulence and the resulting intermittent non-diffusive transport processes. Our previous studies [10-13] have shown that the simulations based on relatively simple adiabatically reduced one-fluid MHD model demonstrate a rather good qualitative and quantitative agreement with many experiments. In particular, the simulations have revealed a number of nontrivial features of turbulent plasma evolutions in mirror based systems. Typically the inverse cascade plays an important role in the nonlinear quasi-2D turbulent plasma evolution. As shown in Ref. [13] this leads to formation of large-scale dominant vortex-like structures, which are rather independent on space scales of the driving linear instability. Therefore, even small-scale instabilities can maintain rather large-scale vortex-like structures in magnetized plasmas. Furthermore, simulations of turbulence and transport in axisymmetric system with internal levitated ring and pure poloidal magnetic field (see Ref. [10-12]) have surprisingly demonstrated many

features previously observed in tokamaks, such as a profile consistency, L-H transitions, etc.. Energy life-times and characteristic times of transients between different confinement regimes were also comparable with the tokamak values. This circumstance gave us an idea to apply our one-fluid turbulence model to simulate the non-diffusive transport in tokamaks. For this purpose we have modified our code CONTRA-C previously designed to simulate 2D turbulence and the resulting transport in cylindrical plasma column with pure poloidal magnetic field. Below the results of first simulations for transient regimes with redistribution of ECH power input and modification of sheared flow profile are presented.

## 2. Basic equations

The basic principles of our transport model have been discussed in details in our previous papers [10-13]. We assume that the plasma is self-consistently maintained in a curved magnetic field near a turbulent-relaxed state which is marginally stable (MS) against an interchange pressure-driven mode. Plasma heating and a background thermal conductivity distort the initial pressure profile making it a weakly unstable. The instability induces and maintains quasi-2D nonlinear convection, which tends to restore the MS pressure profile and results in an anomalous non-diffusive heat transport. The key point of the model is that the cross-field heat and particle fluxes are calculated using fluctuations of pressure, density, and radial velocity obtained by means of direct simulations of turbulent plasma dynamics. Here we discuss cylindrical plasma model.

Similar to the previous considerations we introduce poloidal angle  $\theta$ , "toroidal" angle  $\varphi$  (instead of longitudinal coordinate  $z$ ), major radius  $R$  of an equivalent torus, poloidal magnetic flux function  $\psi$ , and Jacobian  $J$  of the transform to flux coordinates:

$$\varphi = z/R; \quad \psi = R \int_0^r B_p dr; \quad J = [\nabla \varphi \times \nabla \psi] \cdot \nabla \theta.$$

Then we define the specific flux-tube volume:  $U(\psi) = dV(\psi)/(2\pi)^2 d\psi \Rightarrow U = r/B_p = 1/J$ , which does not depend on presence or absence of "toroidal" magnetic field  $B_\varphi$ , and the entropy function  $S = n(T_e + T_i)U^\gamma$ , where the adiabatic index  $\gamma$  characterizes plasma compressibility. Satisfying condition  $dS/dr = 0$  equilibrium plasma pressure profile appears to be marginally stable against interchange flute-like mode in pure poloidal magnetic field. The conventional model of one-fluid MHD with isotropic-pressure assumes that  $\gamma = 5/3$ , however, an effective value  $\gamma \approx 2$  provides better agreement with large aspect ratio tokamak experiments (such as T-10) and the "canonical profile" concept [14, 15]. Therefore, we assume  $\gamma = 2$  in our simulations. Contrary to our previous analysis we account presence of toroidal magnetic field in plasma equilibrium. Grad-Shafranov equation for cylindrical plasma can be written as follows:

$$J(r^2 J)' + 4\pi \bar{p}' + qJR^2(qJ)' = 0; \quad (1)$$

where  $q(r)$  is the conventional tokamak safety factor, bar denotes averaging over magnetic surface, and prime denotes radial derivative. For simplicity Eq. (1) is supplemented by condition  $q = q_0(1 + \alpha_q r^2)$ , where parameters  $q_0$  and  $\alpha_q$  are taken to fit the experimental data.  $\bar{p}$  and  $J$  can slowly vary with time as a result of plasma evolution due to transport processes.

Plasma fluctuations and turbulent velocity field are calculated in the frame of simple but self-consistent one-fluid MHD model with an adiabatically reduced velocity field  $\mathbf{v}_a(t, \psi, \varphi)$  that corresponds to  $E \times B$  plasma convection in pure poloidal magnetic field and takes the form:

$$\mathbf{v}_a(t, \psi, \varphi) = [\mathbf{B}_p \times \nabla \Phi] / B_p^2 \sim \varepsilon c_s, \quad (2)$$

where function  $\Phi(t, \psi, \varphi)$  has the meaning of 2D electric potential. We understand that the formal independence of convection on toroidal magnetic field looks a little bit strange, nevertheless, due to a similarity of the main constrains such simplified plasma dynamics allow us to obtain very reasonable results. Small parameter  $\varepsilon$  determines level of fluctuations in the well-developed turbulence and is defined by the following relation:  $\varepsilon^3 \sim \chi / c_s a$ , where  $\chi$  is a background local thermal diffusivity,  $c_s$  is the sound speed, and  $a$  is a minor radial scale.

The entropy function consists of surface-averaged slow varying function  $\bar{S}$ , which is determined by  $\bar{p} = \bar{S}(t, \psi) J^\gamma$ , and small fluctuating component  $\tilde{S}(t, \psi, \varphi)$ :

$$S = \bar{S}(t, \psi) + \tilde{S}(t, \psi, \varphi); \quad \tilde{S} \sim \varepsilon^2 \bar{S}; \quad |\nabla \bar{S}| \sim \varepsilon^2 \bar{S} / a^2 \quad (3)$$

Heat transfer equation that determines the function  $\bar{S}(t, \psi)$  has the form:

$$\partial_t \bar{S} \Big|_\psi + \partial_\psi (\overline{\tilde{S} \partial_\varphi \Phi}) = \frac{2}{3} \frac{R^2}{J^{\gamma-1}} \partial_\psi \left( r^2 J \bar{\rho} \bar{\chi} \partial_\psi \frac{\bar{S} J^\gamma}{\bar{\rho}} \right) + \frac{2}{3} \frac{\bar{Q}_E}{J^\gamma}, \quad (4)$$

where the second term in the left-hand-side describes turbulent non-diffusive transport and the energy source includes ECH heating, ohmic heating (OH), viscous heating due to turbulence dissipation, and radiation losses:

$$\bar{Q}_E = \bar{Q}_{ECH} + \bar{Q}_{OH} + \bar{Q}_{viscous} - \bar{Q}_{rad}. \quad (5)$$

In simulations presented here we assume completely turbulent-relaxed mass-density profile ( $\bar{\rho} U = const$ ) and neglect by density fluctuations. Equations for fluctuations consist of equation for  $\tilde{S}(t, \psi, \varphi)$  and dynamic equation for vorticity of flux-tube  $w = U \nabla \cdot (\nabla \Phi / C_A^2)$ :

$$\partial_t \tilde{S} + [\Phi, \tilde{S}] - \partial_\psi (\overline{\tilde{S} \partial_\varphi \Phi}) + \partial_\varphi \Phi \partial_\psi \bar{S} = \frac{U^2}{3} \nabla \cdot \left( \bar{\rho} \bar{\chi} c_s \nabla (c_s \frac{\tilde{S}}{\bar{S}}) \right), \quad (6)$$

$$\partial_t w + [\Phi, w] + \frac{1}{U^\gamma} \partial_\psi U \partial_\varphi \tilde{S} = U \nabla \cdot \left( \frac{\nabla (\bar{\eta} C_A^2 w)}{C_A^2} \right) + Q_w, \quad (7)$$

where  $[\Phi, w] = \partial_\varphi \Phi \partial_\psi w - \partial_\psi \Phi \partial_\varphi w$ ,  $\eta$  is a background viscosity, and  $Q_w$  is vorticity source.

### 3. Results of simulations.

Self-consistent plasma convection and the resulting transport processes in cylindrical plasma column were simulated as an evolutionary problem with given initial and boundary conditions. The initial conditions were chosen to correspond to parameters of tokamak T-10, namely to parameters of shot No 33965. The toroidal magnetic field is  $B_\varphi = 2.5 T$ , the major plasma radius is  $R = 150 cm$ , the minor radius (restricted by diaphragm) is  $r_d = 30 cm$ , surface  $q = 1$  has the radius  $r_c \approx 10 cm$ . On axis plasma density, electron and ion temperatures have the following values:  $n_0 = 6.23 \times 10^{13} cm^{-3}$ ,  $T_{e0} = 2.075 keV$ ,  $T_{i0} = 0.767 keV$ . Plasma core is negatively charged and typical radial potential difference is  $\Delta \Phi \approx 100 V$ .

In our simulations we assume that the turbulent fluctuations exist in the region between the surface  $q = 1$  and the diaphragm ( $r_c \leq r \leq r_d$ ) and vanish at the both radial boundaries. All functions are periodic functions of "toroidal" angle  $\varphi$ . According to Eq. (4) the total heat flux at the surface  $r = r_c = 10 cm$  has to be completely determined by the background thermal

diffusivity  $\chi$ . Experimental data analysis shows that both electrons and ions have almost the same effective  $\chi$ -values at  $r = r_s$  and this value approximately corresponds to the ion neoclassical value. Therefore, we assume that the background  $\chi$  has neoclassical radial scaling and  $\chi(r_c) = 0.9m^2/s$ . Small parameter  $\varepsilon$  calculated at  $r = r_c$  has the value  $\varepsilon_{\text{exp}} = 2.685 \cdot 10^{-2}$  in the shot No 33965. However, solving the set of equations for turbulent fluctuations and plasma heat transport in dimensionless form we used  $\varepsilon = 0.1$  or  $\varepsilon = 0.05$  to accelerate computations and then rescaled the dimensionless time unit to real experimental time scale. Below we present results of computations with  $\varepsilon = 0.1$ . Total dimensionless time of computations ( $t = 400$ ) corresponds approximately to  $44.5 \text{ ms}$  for  $T=10$  conditions.

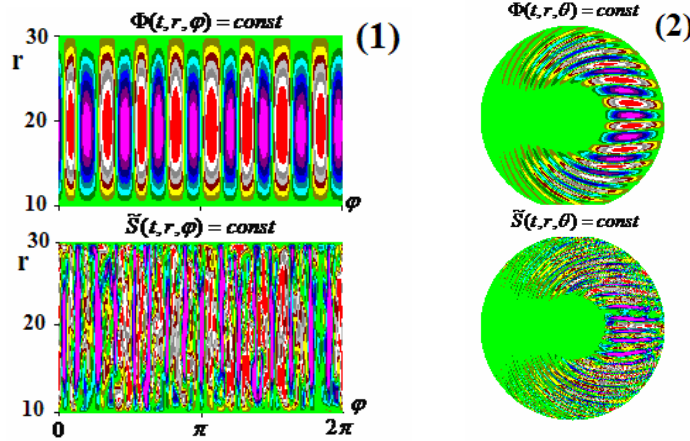


FIG. 1. Levels of plasma potential fluctuations  $\Phi = \text{const}$  and fluctuations of entropy  $\tilde{S} = \text{const}$  in equatorial cross-section (1) and in poloidal cross-section (2) in the standard regime (a).

Three different regimes of plasma confinement have been simulated. Regime (a) corresponds to non-modified conditions of shot No 33965. We assume the following energy sources in Eq. (5). ECH power input is a dominant part of the total power input:  $\overline{Q}_{ECH} = 0.9\overline{Q}_{tot}$ . It is localized near the surface  $r_{\text{hl}} = 12.5 \text{ cm}$  with a half-width  $2.5 \text{ cm}$ .  $\overline{Q}_{OH} = 0.1\overline{Q}_{tot}$  is distributed mainly in the region  $r \leq r_c$ . Radiation losses  $\overline{Q}_{rad} = 0.1\overline{Q}_{tot}$  rise parabolically to the edge. The viscous heating depends on turbulence evolution. Fig. 1 illustrates structure of well-developed turbulence in regime (a). Fig.1(1) represents levels of potential  $\Phi(t, r, \varphi) = \text{const}$  or lines of turbulent flows including zonal flows and levels of entropy fluctuations  $\tilde{S}(t, r, \varphi) = \text{const}$  in the moment  $t = 400$ . Warm colors correspond to positive values of the functions. These functions are directly calculated using Eqs. (6) and (7). From the other hand-side, we can consider Fig.1(1) as projections of the fluctuations onto the equatorial cross-section ( $(r, \varphi)$ -plots) of the equivalent torus at the low-field side ( $\theta = 0$ ). To show fluctuations in a more familiar form we project the fluctuations along tokamak field-lines  $\varphi - q(r)\theta = \text{const}$  onto poloidal cross-section  $\varphi = 0$  assuming presence of toroidal magnetic field and a "ballooning effect" that provides a smooth fluctuation vanishing at the high-field side ( $\theta = \pm\pi$ ). Projections of fluctuations onto the poloidal cross-section ( $(r, \theta)$ -plots) correspond to an expected poloidal structure of fluctuations in real tokamak geometry and are shown at Fig.1(2). It is seen from Fig. 1(2) that the fluctuations look similar to those obtained in gyrokinetic simulations [1, 2] and that the spacial structures of  $\Phi(t, r, \theta)$  and  $\tilde{S}(t, r, \theta)$  (including dominant  $m$ -numbers) are appreciably different from each other, because they are generated by a strong turbulence.

Regime (b) has the same initial conditions, total integral power input  $\int \bar{Q}_{tot} r dr$ , and radial potential difference  $\Delta\Phi \approx 100 V$  as in the regime (a), however, in a particular moment  $t = 100$  a significant part of the initial ECH power (40–90% of  $\bar{Q}_{ECH}$ ) is switched to another gyrotron that provides power input with a half-width 1.25 cm near the surface  $r_{h2} = 25 cm$ . The switching is accompanied by the corresponding reduction of power input near  $r_{h1} = 12.5 cm$ . The gyrotrons for the realization of regime (b) are available in T-10 experiments. Regime (c) models an influence of possible shear-flow drive when a picked vorticity (i.e. layer of high toroidal velocity shear) is artificially maintained near a surface  $r_w = 17 cm$ . In this regime radial potential difference rises to  $\Delta\Phi \approx 400 V$  providing a faster plasma rotation.

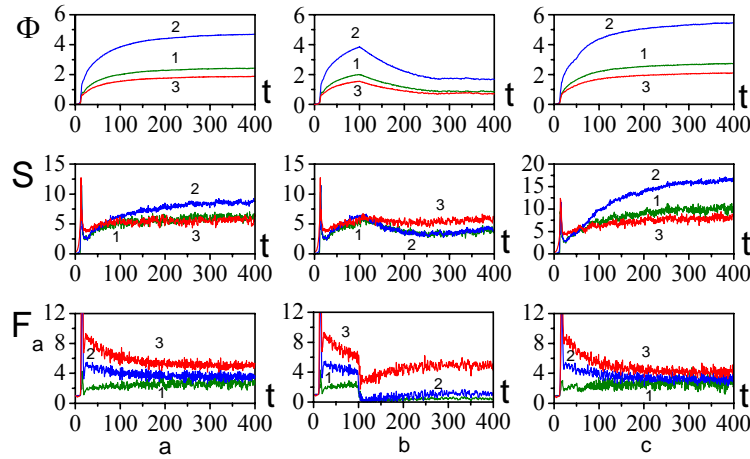


FIG.2. Levels of fluctuations of potential  $\Phi$ , entropy  $S$ , and anomaly factor  $F_a$  averaged over three magnetic surfaces: 1 – surface  $r_1 = 13 cm$ ; 2 – surface  $r_2 = 20 cm$ ; 3 – surface  $r_3 = 27 cm$ .

Fig.2 shows evolutions of surface-averaged fluctuations of potential  $\Phi$  and entropy  $S$  (more precisely square roots of surface-averaged square values of fluctuations:  $(\overline{\Phi^2})^{1/2}$  and  $(\overline{S^2})^{1/2}$ ), and the anomaly factor  $F_a$ , which is defined as a ratio of total (anomaly) surface-averaged heat flux to the back-ground (neoclassical) heat flux:  $F_a = q^{an} / q^{ncl}$ . Fig.2a represents the standard regime (a). It is seen that after  $t \approx 20$  ( $\sim 2 ms$ ) the first relatively fast transient, which includes a gross due to linear instability and an initial formation of nonlinear turbulent structures, transforms to a stage of well-developed turbulence that slow evolves with a characteristic time that is comparable with the energy life-time  $\tau_E \approx 30 ms$ . Here and below the energy life-time is defined as ratio of integral plasma thermal energy to the total integral power input.

Fig.2b represents regime (b) with 60% of  $\bar{Q}_{ECH}$  switched to the second gyrotron at  $t = 100$ . After the ECH power redistribution the anomaly factor  $F_a$  drops down dramatically at all radii with very short transient time  $\Delta t \sim 4-5$  ( $\sim 0.5 ms$ ) while the fluctuation levels decrease gradually (with characteristic time  $\sim \tau_E$ ). This means that the convective heat flux changes mainly due to a fast change of phase relations between fluctuations  $\tilde{\Phi}$  and  $\tilde{S}$  rather than due to a decrease of fluctuation level. In the core region (curves 1 and 2 in Fig.2b) the anomaly factor  $F_a$  drops down even below 1 just after the ECH power redistribution and it is still essentially reduced later while  $F_a$  at the edge (at  $r_3 > r_{h2}$ ) restores its value to a level that is

comparable with the level of  $F_a$  in regime (a) (compare curves 3 in Fig.2b and Fig.2a). This indicates that the convective heat flux in regime (b) is appreciably reduced in the core region and even can temporarily takes an inverse value. This result is similar to heat flux reductions in ASDEX experiments with the ECH power redistribution (see Fig. 3 in Ref. [16]).

Fig. 2c represents regime (c) in which the high-vorticity layer is maintained by a source of vorticity  $Q_w$  in Eq. (7) localized near a surface  $r_w = 17 \text{ cm}$ . The evolution looks similar to those in regime (a), however, level of fluctuations near the surface  $r_2 = 20 \text{ cm}$  (curves 2 in Fig.2c) is an appreciably enhanced presumably due to an influence of Kelvin-Helmholtz instability. Making simulations in regime (c) we expected to form an internal transport barrier (ITB) in the vicinity of high-vorticity layer. Such ITB was observed in GAMMA 10 tandem mirror experiments [8,9] and its formation was demonstrated in our previous simulations for mirror geometry [13]. Unfortunately, we have not obtained an ITB in modern tokamak-related simulations up to now. Nevertheless, Fig. 2c shows that the anomaly factor  $F_a$  is reduced in regime (c) (especially at the edge at  $r_3 = 27 \text{ cm}$ ) in comparison with the regime (a) in spite of the enhanced level of fluctuation near the surface  $r_2 = 20 \text{ cm}$ .

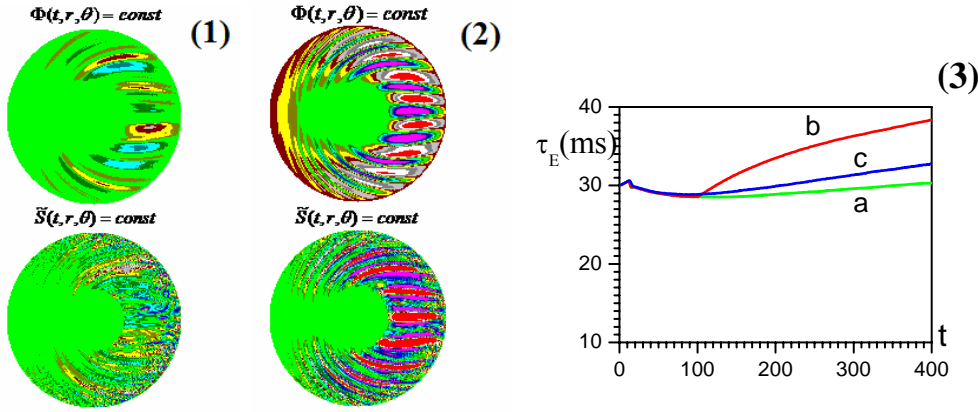


FIG. 3. 1 – plasma fluctuations in regime (b); 2 – plasma fluctuations in regime (c); 3 – evolution of the energy life-time  $\tau_E$  in regimes (a), (b), and (c).

Fig. 3 shows fluctuations in regimes (b) and (c) in the moment  $t=400$ . Fig. 3(1) demonstrates the appreciable reduction of fluctuations in the core region in comparison with the Fig. 1(2) that agrees with the data presented at Fig. 2b and Fig. 2a. Curve (b) in Fig. 3(3) shows that the energy life-time  $\tau_E$  in the regime (b) appreciably rises after switching of 60% of ECH power input to  $r_{h2} = 25 \text{ cm}$  and exceeds the life-time in regime (a) by 27% at  $t=400$ . This result is a little bit surprising from the view point of the conventional diffusive transport theory, but it is very reasonable for the discussed turbulence model, because the anomaly factor  $F_a$  is essentially reduced over the wide radial range in the regime (b) while the level of turbulence is still sufficiently high to maintain the pressure profile near the turbulent-relaxed state (see discussion of Fig. 4 below). 60% of  $\bar{Q}_{ECH}$  looks as a reasonable value for the switching, because the further enhancement of switched ECH power up to 70% or greater results in a flattening of pressure profile in the core region and cases almost complete suppression of the core turbulence. The flattening of pressure profile prevents the further rise of  $\tau_E$ . The regime (b) can be classified as a non-standard L-H transition without formation of an external transport barrier.

Fig. 3(2) shows that maintenance of the high vorticity layer near the surface  $r_w = 17 \text{ cm}$  appreciably modifies the turbulent structures in the regime (c) in comparison with the regime (a). Higher vorticity cases enhancement of fluctuation level in the core plasma ( $r < 25 \text{ cm}$ ) and reduces poloidal  $m$ -numbers of the dominant turbulent structures while the fluctuations at the edge ( $r > 25 \text{ cm}$ ) have moderate amplitudes and maintain a reduced anomaly factor  $F_a$  (see Fig. 2(c)). As a result curve (c) in Fig. 3(3) shows an increase of  $\tau_E$  in comparison with the regime (a).

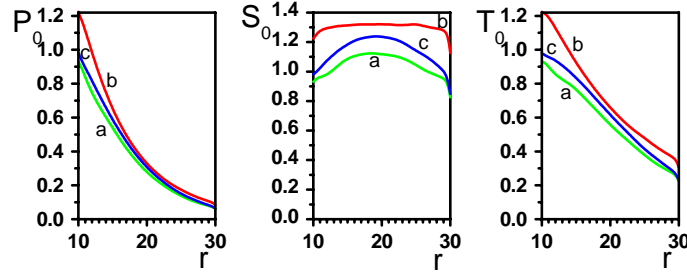


FIG. 4. Profiles of plasma pressure  $P_0$ , entropy  $S_0$ , and temperature  $T_0$  in regimes (a), (b), and (c).

Fig.4 presents profiles of plasma pressure  $P_0$ , entropy function  $S_0$ , and temperature  $T_0$  at the moment  $t = 100$ . The highest pressure and temperature were achieved in regime (b). The pressure profile in this regime is maintained closely to the turbulent-relaxed state  $S_0 = const$  which can be considered as the "canonical" pressure profile for our model. We could compare our  $T_0$ -profiles with  $T_e$ -profiles in sawtooth-free discharges in ASDEX shown at Fig. 6 of Ref. [16]. The relative enhancement of  $T_0$  in the core region in our regime (b) is higher than that in the experiments with ratio 25/75 for ECH power input (see Fig. 6 in Ref. [16]). However, we guess that this difference appears due to some simplified assumptions. We should remind that our simulations were performed in the frame of one-fluid MHD model. Therefore the temperature  $T_0$  is a "common" temperature ( $T_0 = T_e + T_i$ ) with a fixed ratio  $T_e/T_i$  for all times and radii. Further, we have assumed that the density profile satisfies the condition of complete turbulent relaxation ( $\bar{\rho}U = const$ ) while the density profiles in the experiments with the strong ECH in the plasma core typically demonstrate a relative density decrease in the core region in comparison with the profile  $\bar{\rho}U = const$ . Being accounted in simulations of regime (a) such the decrease would be compensated by the corresponding temperature increase under the condition of pressure profile conservation. We intend to account density fluctuations and modifications of density profiles in our simulations later. The entropy in regime (c) has a hump profile with the greatest deviations (up to 10%) from the profile  $S_0 = const$ . Decrease of  $S_0$  at the edge in this regime results in enhanced relative gradients of pressure and temperature for  $r > 23 \text{ cm}$ . The tendency of gradient enhancement is similar to that was observed in a "transport barriers", however, it is not sufficiently high in our simulations. We intend to continue our simulations of shear-flow influence.

#### 4. Summary

Quasi-2D plasma turbulence and the associated cross-field heat transport in a cylindrical model of tokamak have been simulated for T-10 conditions. Modified version of code CONTRA-C based on adiabatically reduced one-fluid MHD was used in the simulations. Two

different scenarios of transitions to improved confinement regimes were analyzed and simulated numerically. The first scenario has demonstrated the considerable reduction of turbulence and cross-field heat transport after redistribution of 40-90% of ECH power input closer to the plasma edge. This result does not contradict to earlier ASDEX experiments and can be verified in T-10 experiments. Controlled modification of sheared flow profile was simulated in the second scenario. It is shown that the presence of high vorticity layer in the sheared flow profile can appreciably modify the structure of LF turbulence leading to a decrease of cross-field transport and enhancement of plasma energy life-time. This result qualitatively agrees with experimental observations, however, additional simulations are necessary for a more detailed comparison with tokamak experiments.

In general, the results obtained have shown that the simulations based on relatively simple adiabatically reduced one-fluid MHD model could be considered as a reasonable method of theoretical study of quasi-2D structured turbulence and the resulting intermittent non-diffusive transport processes in tokamak plasmas.

We are glad to acknowledge very fruitful discussions with N.A. Kirneva, Yu.N. Dnestrovskij, and K.A. Rasumova. The work was supported in part by Russian Foundation for Basic Research (Grant 07-02-00583) and by Grant 2457.2008.2 for support of leading scientific schools in Russian Federation.

## References

- [1] TERRY, P.W., *Reviews of Modern Physics* **72** (2000) 109.
- [2] DIAMOND, P.H., et al., *Plasma Phys. Control. Fusion* **47** (2005) R35.
- [3] WADE, M. R. and DIII-D Team, *Nucl. Fusion* **47** (2007) S543.
- [4] TAKENAGA, H. and JT-60 Team, *ibid.* **47** (2007) S563.
- [5] GRUBER, O. for the ASDEX Upgrade team, *ibid.* **47** (2007) S622.
- [6] YAMADA, H., et al., *ibid.* **45**, (2005) 1684.
- [7] MOTOJIMA, O., et al., *ibid.* **47**, (2007) S668.
- [8] CHO, T., et al., *Phys. Rev. Letters* **97** (2006) 055001.
- [9] CHO, T., et al., *Phys. Plasmas* **15** (2008) 056120.
- [10] PASTUKHOV, V.P., and CHUDIN, N.V., *Plasma Phys. Reports* **27** (2001) 907.
- [11] PASTUKHOV, V.P., and CHUDIN, N.V., "Nonlinear 2D Convection and Enhanced Cross-Field Plasma Transport Near the MHD Instability Threshold", *Fusion Energy 2002 (Proc. 19th Int. Conf. Lyon, 2002)*, C&S Papers Series No. 19/C, IAEA, Vienna (2003), CD-ROM file TH2\_5.
- [12] PASTUKHOV, V.P., and CHUDIN, N.V., *JETP Letters* **82** (2005) 356.
- [13] PASTUKHOV, V.P., and CHUDIN, N.V., *Transactions of Fusion Science and Technologies* **51** (2007) 34.
- [14] RASUMOVA, K.A., et al., *Plasma Phys. Control. Fusion* **48** (2006) 1373.
- [15] RASUMOVA, K.A., et al., *ibid.* **50** (2008) 105004.
- [16] RYTER, F., et al., *Nucl. Fusion* **43** (2003) 1396.